p s s b

physica status solidi

www.pss-b.com

basic solid state physics

Feature Article

Coupled magnetic plasmons in metamaterials

H. Liu[*, 1]**, Y. M. Liu**[2]**, T. Li**[1]**, S. M. Wang**[1]**, S. N. Zhu**[1]**, and X. Zhang**[2, 3]

[1] Department of Physics, Nanjing University, Nanjing 210093, P.R. China
[2] Nanoscale Science and Engineering Center, University of California, 5130 Etcheverry Hall, Berkeley, CA 94720-1740, USA
[3] Materials Sciences Division, Lawrence Berkeley National Laboratory, 1 Cycletron Road, Berkeley, CA 94720, USA

* Corresponding author: e-mail liuhui@nju.edu.cn, URL: http://dsl.nju.edu.cn/dslweb/images/plasmonics-MPP.htm

Magnetic metamaterials consist of magnetic resonators smaller in size than their excitation wavelengths. Their unique electromagnetic properties were characterized by the effective media theory at the early stage. However, the effective media model does not take into account the interactions between magnetic elements; thus, the effective properties of bulk metamaterials are the result of the "averaged effect" of many uncoupled resonators. In recent years, it has been shown that the interaction between magnetic resonators could lead to some novel phenomena and interesting applications that do not exist in conventional uncoupled metamaterials. In this paper, we will give a review of recent developments in magnetic plasmonics arising from the coupling effect in metamaterials. For the system composed of several identical magnetic resonators, the coupling between these units produces multiple discrete resonance modes due to hybridization. In the case of a system comprising an infinite number of magnetic elements, these multiple discrete resonances can be extended to form a continuous frequency band by strong coupling. This kind of broadband and tunable magnetic metamaterial may have interesting applications. Many novel metamaterials and nanophotonic devices could be developed from coupled resonator systems in the future.

1 Introduction All classical electromagnetic (EM) phenomena in various media are determined by the well-known Maxwell's equations. To describe the EM properties of a material, two important parameters are introduced, that is, electric permittivity ε and magnetic permeability μ. In principle, if the ε and of materials are known, then the propagation of EM waves inside materials, or the EM phenomena at the surface between two materials can be well predicted. For example, the refraction of an EM wave at the interface is described by Snell's law, $\sin\theta_i / \sin\theta_r = n_r/n_i$, which states that the relation between the incident angle (θ_i) and the refracted angle (θ_r) is determined by the refractive index, $n = \sqrt{\varepsilon\mu}$, of the two media involved.

Clearly, if we can modify ε and μ artificially, then the propagation behavior of EM waves in the material can be manipulated at will. For instance, in 1967 when Veselago first theoretically studied the EM properties of a material with a negative refractive index (simultaneously negative ε and μ), he found that light will be refracted negatively at the interface between such a material and a normal positive index material [1]. This so-called "negative refraction" phenomenon does not violate the laws of physics, yet it challenges our physical perception and intuition. In such negative index media (NIM), a number of other surprising phenomena were also predicted, such as the reversed Doppler shift and Cerenkov radiation. However, Veselago's work was ignored for a long time because no such double negative materials (i.e., where both $\varepsilon < 0$ and $\mu < 0$) are obtainable in nature, making negative refraction seemingly impossible. Indeed, we are limited by the natural material properties. Most dielectrics only have positive permittivities. For most metals, $\varepsilon < 0$ can be met at optical range, and the plasma frequency can be moved downwards into microwave range by replacing the bulk metal with a rodded medium [2–4], yet permeability is always positive. Negative μ is accessible in some ferromagnetic materials in the microwave region, but they are diffi-

WILEY InterScience®
DISCOVER SOMETHING GREAT

cult to find above terahertz frequencies in the natural world.

In recent years, to achieve designable EM properties, especially negative μ at high frequencies, people have invented novel artificial materials known as metamaterials. The basic idea of a metamaterial is to design artificial elements that possess electric or magnetic responses to EM waves. Many such elements can work as artificial "atoms" to constitute a metamaterial "crystal". The geometric size of these atoms and the distances between them are much smaller than the wavelength of EM waves. Then, for an EM wave, the underlying metamaterial can be regarded as a continuous "effective medium". Correspondingly, the property of a metamaterial can be described by two effective parameters: effective permittivity ε_{eff} and permeability μ_{eff}. In 1999, Pendry first designed a metallic magnetic resonance element: a split-ring resonator (SRR) [5]. When an SRR is illuminated by light, the magnetic component of the EM wave induces the faradic current in this structure, giving rise to a magnetic dipole. Using SRRs as structure elements, Pendry constructed a new kind of magnetic metamaterial. The effective permeability, μ_{eff}, of this metamaterial has the form

$$\mu_{\text{eff}} = 1 - \frac{F\omega^2}{\omega^2 - \omega_{mp}^2 + i\gamma\omega}, \tag{1}$$

where F is the fractional volume of the cell occupied by the SRR. Equation (1) suggests that μ_{eff} follows a Drude–Lorentz resonance, and μ_{eff} can be negative around the frequency ω_{mp} if the damping term γ is not so large. Such plasmon resonance in SRR is caused by a magnetic field, so the corresponding resonance frequency, ω_{mp}, here is called the magnetic plasmon (MP) frequency. Motivated by Pendry's work, Smith combined SRR and metallic wires to construct a metamaterial with simultaneously negative ε_{eff} and μ_{eff} [6]. The negative refraction proposed by Veselago was finally experimentally verified in the microwave region [7].
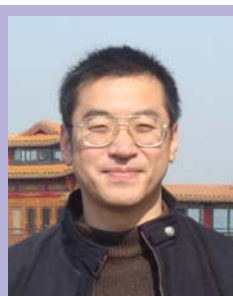
Hui Liu received his Ph.D. in Condensed Matter Physics from the Department of Physics of Nanjing University, China, in 2003. His doctor thesis concerned nonlinear optical properties of dielectric superlattices. In 2004–2005 he did postdoctoral research at the Nanoscale Science and Engineering Center, University of California at Berkeley, where he was working on magnetic plasmons in metamaterials. Since 2006, he has been Associate Professor of Physics at Nanjing University in China. Currently, the subject of his studies is the various interesting properties introduced by hybridization effect in coupled metamaterials.

One of the most important applications of NIMs is a superlens, which allows imaging resolution beyond the diffraction limit [8–13]. Considering its significant applications in the visible region, increasing the MP frequency, ω_{mp}, to obtain negative refraction for visible light is a very valuable and challenging task. Given that ω_{mp} arises from an inductor-capacitor circuit (LC) resonance in SRRs and is determined by the geometric size of this structure, it can be increased by shrinking the size of the SRRs. In 2004, Zhang and colleagues fabricated a planar structure composed of SRRs. The size of the SRR was just a few micrometers, and ω_{mp} was around 1 THz [14]. Immediately after Zhang's work, Soukoulis and colleagues fabricated an SRR sample with a unit cell of several hundred nanometers, and ω_{mp} was raised to 100 THz [15]. Another result is obtained around 1.5 μm, which is the telecommunication wavelength in the infrared range [16]. As the structure of an SRR is so complex, it is very difficult to decrease its geometric size any further with the existing nanofabrication technique. To obtain MP resonance at higher frequencies, people began to seek other simple MP structures. In fact, inductive coupled rod pairs are very simple structures that Zheludev and colleagues proposed as constituting chiral metamaterials [17]. Shalaev and colleagues found that such nanorod pairs could also be used to produce MP resonance and negative refraction at the optical communication wavelength of 1.5 μm [18, 19]. Almost at the same time, Zhang et al. proposed a double-fishnet structure to obtain negative refraction at about 2 μm [20]. Although Shalaev and Zhang verified that their structures possessed a negative refraction index by measuring the phase difference of the transmitted waves, they could not directly observe the negative refraction in their monolayer metamaterial structures. Until quite recently, direct negative refraction was observed by Zhang and colleagues in the three-dimensional bulk metamaterials of nanowires [21] and fishnet structures [22] in the optical region. Besides the aforementioned important works on negative refraction, many other studies from recent years provide a good introduction to the rapid progress that has taken place in this field [23–27]. In addition to negative refractions, MP resonance has also been applied to another metamaterial that has attracted considerable attention, namely, cloaking materials [28–30].

Although the invention of the metamaterial has stimulated the interest of many researchers and its various applications have been widely discussed, the basic design idea is very simple: composing effective media from many small structured elements and controlling its artificial EM properties. According to the effective-media model, the coupling interactions between the elements in metamaterials are somewhat ignored; therefore, the effective properties of metamaterials can be viewed as the "averaged effect" of the resonance property of the individual elements. However, the coupling interaction between elements should always exist when they are arranged into metamaterials. Sometimes, especially when the elements are very
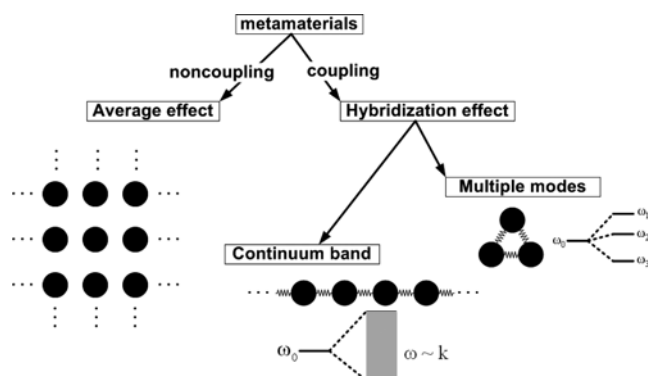
Feature

Article

Phys. Status Solidi B **246**, No. 7 (2009)   1399

Figure 1 "Average effect" and "hybridization effect" in metamaterials.

Figure 2 (online colour at: www.pss-b.com) (a) Structure of a magnetic dimer; (b) equivalent LC circuit.

close, this coupling effect is not negligible and will have a substantial effect on the metamaterial's properties. Under such circumstances, the uncoupling model is no longer valid, and the effective properties of the metamaterial cannot be regarded as the outcome of the averaged effect of a single element (see Fig. 1). Many new questions arise: How do we model the coupling in metamaterials? What new phenomena will be introduced by this coupling effect? Can we find any new interesting applications in these coupled systems?

Magnetic metamaterials consisting of resonance elements with a strong coupling interaction have already developed into an important branch of metamaterial research. The "hybridization effect" caused by these coupling interactions between magnetic resonators in metamaterials is attracting increased interest. Some multiple hybrid modes or continuum collective MP modes were found in magnetic metamaterials after including this hybridization effect (see Fig. 1). Quite a number of papers have already reported this new kind of coupled MP resonance modes. Various novel phenomena and properties have been explored, and these have led to many new interesting applications that do not exist in uncoupled metamaterials. In this review paper, we will give an overall introduction to these recent developments in MP modes that were introduced by the coupling effect in metamaterials. First, the hybridization effect of MP resonance in two coupled magnetic resonators is presented in section two. Second, we will describe the MP propagation waves in a one-dimensional chain of magnetic resonators in Section 3. Then, the excitation of MP in a two-dimensional (2-D) coupled system will be discussed in section four. In the last section, an outlook will be presented to predict possible future developments of coupled MP modes in metamaterials.

2 Hybrid magnetic plasmon modes in metamaterials In 2003 [31], Halas and colleagues introduced a hybridization model to describe the plasmon response of complex nanostructures. It was shown that the resonance modes of a complex metallic nanosized system could be understood as the interaction or hybridization result of the
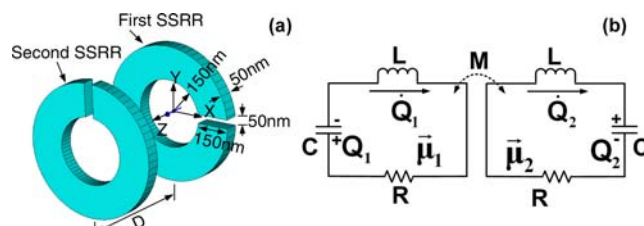
elementary geometries. The hybridization principle provides a simple conceptual approach to designing nanostructures with desired plasmon resonances. In their following work, this method was successfully used to describe the plasmon resonance in a nanoshell [32], nanoparticle dimers [33], nanoshell dimers [34, 35], and nanoparticles near metallic surfaces [36].

In fact, the hybridization model could also be applied to deal with the EM wave response of metamaterials that comprise many resonance elements. SRR is the best-known magnetic "atom" of metamaterials. Therefore, the investigation of how SRRs interact with each other is both a fundamental and typical study. Apparently, a magnetic dimer (MD) made of two SRRs is the simplest system with which to study the coupling effect [37]. In Fig. 2, we present the general configuration of an MD, composed of two identical SRRs separated by a finite distance, D. To study the magnetic response of this MD, an MP hybridization model was established. In our approach, we use the Lagrangian formalism, first calculating the magnetic energy of a single SRR and later expanding the theory for a system of two coupled SRRs. For simplicity, in the analysis we consider each SRR an ideal LC circuit composed of a magnetic loop (the metal ring) with inductance L and a capacitor with capacitance C (corresponding to the gap). The resonance frequency of the structure is given by $\omega_0 = 1/\sqrt{LC}$, and the magnetic moment of the SRR originates from the oscillatory behavior of the currents induced in the resonator. If we define the total charge, Q, accumulated in the slit as a generalized coordinate, the Lagrangian corresponding to a single SRR is written as $\Im = L\dot{Q}^2/2 - Q^2/2C$, where $\dot{Q}$ is the induced current, $L\dot{Q}^2/2$ relates to the kinetic energy of the oscillations, and $Q^2/2C = L\omega_0^2 Q^2/2$ is the electrostatic energy stored in the SRR's gap. Similarly, the Lagrangian that describes the MD is a sum of the individual SRR contributions with an additional interaction term

$$\Im = \frac{L}{2}\left(\dot{Q}_1^2 - \omega_0^2 Q_1^2\right) + \frac{L}{2}\left(\dot{Q}_2^2 - \omega_0^2 Q_2^2\right) + M\dot{Q}_1\dot{Q}_2 , \qquad (2)$$

where Q_i ($i = 1, 2$) are the oscillatory charges and M is the mutual inductance. By substituting $\Im$ in the Euler–Lagrange equations

$$\frac{d}{dt}\left(\frac{\partial \Im}{\partial \dot{Q}_i}\right) - \frac{\partial \Im}{\partial Q_i} = 0 \quad (i = 1, 2) , \qquad (3)$$
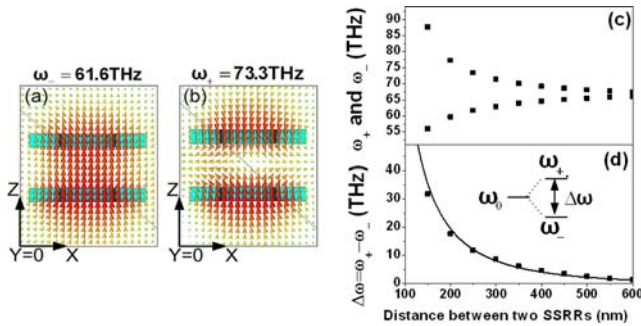
Figure 3 (online colour at: www.pss-b.com) Local magnetic field profiles for the (a) bonding and (b) antibonding MP modes. The dependence of the resonance frequencies (c) and the frequency gap (d) on the distance between two SRRs.

it is straightforward to obtain the magnetic plasmon eigenfrequencies, $\omega_{+/-} = \omega_0 / \sqrt{1 \mp \kappa}$, where $\kappa = M/L$ is a coupling coefficient. The high energy or anti-bonding mode, $|\omega_+\rangle$, is characterized by anti-symmetric charge distribution ($Q_1 = -Q_2$), while the opposite is true for the bonding or low energy $|\omega_-\rangle$ magnetic resonance ($Q_1 = Q_2$). Naturally, the frequency split $\Delta\omega = \omega_+ - \omega_- \approx \kappa\omega_0$ is proportional to the coupling strength. The hybridization of the magnetic response in the case of a dimer is mainly due to inductive coupling between the SRRs. If each SRR is regarded as a quasi-atom, then the MD can be viewed as a hydrogen-like quasi-molecule with energy levels ω_- and ω_+ originating from the hybridization of the original (decoupled) state, ω_0. The specific nature of the MP eigenmodes is studied in Fig. 3 in which the local magnetic field distributions are depicted for the low energy (ω_-) and high energy (ω_+) states respectively. In accordance with the prediction based on the Lagrangian approach, the SRRs oscillate in-phase for the bonding mode $|\omega_-\rangle$ and out of phase for the anti-bonding mode $|\omega_+\rangle$. Since the mutual inductance M decreases dramatically with distance, a strong change in the resonance frequencies $\omega_\pm$ is expected. This phenomenon is demonstrated in Fig. 3(c)–(d), where the MP eigenfre-

quencies $\omega_\pm$ and the frequency change $\Delta\omega = \omega_+ - \omega_-$ are calculated. With a decreasing separation between the SRR, an increase in the frequency gap $\Delta\omega$ is observed. The opposite effect takes place at large distances where the magnetic response is decoupled. This result has already been experimentally proven in the microwave range [38].

Recently, the coupling mechanism between two stacked SRRs was found not only to be determined by the distance between the two elements, but also to depend on the relative twist angle, φ [39]. The Lagrangian of such a twisted structure is a combination of two individual SRRs with the additional electric and magnetic interaction terms

$$\Im = \frac{L}{2}\left(\dot{Q}_1^2 - \omega_0^2 Q_1^2\right) + \frac{L}{2}\left(\dot{Q}_2^2 - \omega_0^2 Q_2^2\right) + M_H \dot{Q}_1 \dot{Q}_2$$
$$- M_E \omega_0^2 Q_1 Q_2 \left(\cos\phi - \alpha\left(\cos\phi\right)^2 + \beta\left(\cos\phi\right)^4\right). \quad (4)$$

In fact, magnetic and electric coupling coexist in the system when $\varphi \neq 90°, 270°$. When φ is changed, although magnetic coupling maintains the same value, electric coupling will change significantly (see Fig. 4). Magnetic and electric interactions contribute oppositely and positively for $\varphi = 0°$ and $180°$ twisted structures respectively. By solving the Euler–Lagrange equations, the eigenfrequencies of these coupled systems can be obtained as

$$\omega_\pm = \omega_0 \sqrt{\frac{1 \mp \kappa_E \left(\cos\phi - \alpha\left(\cos\phi\right)^2 + \beta\left(\cos\phi\right)^4\right)}{1 \mp \kappa_H}}, \quad (5)$$

where $\kappa_E = M_E/L$ and $\kappa_H = M_H/L$ are the coefficients of the overall electric and magnetic interactions respectively. These results lead to an exciting new concept of plasmonic structures: stereometamaterials, which will have profound application potentials in biophotonics, pharmacology, as well as diagnostics.
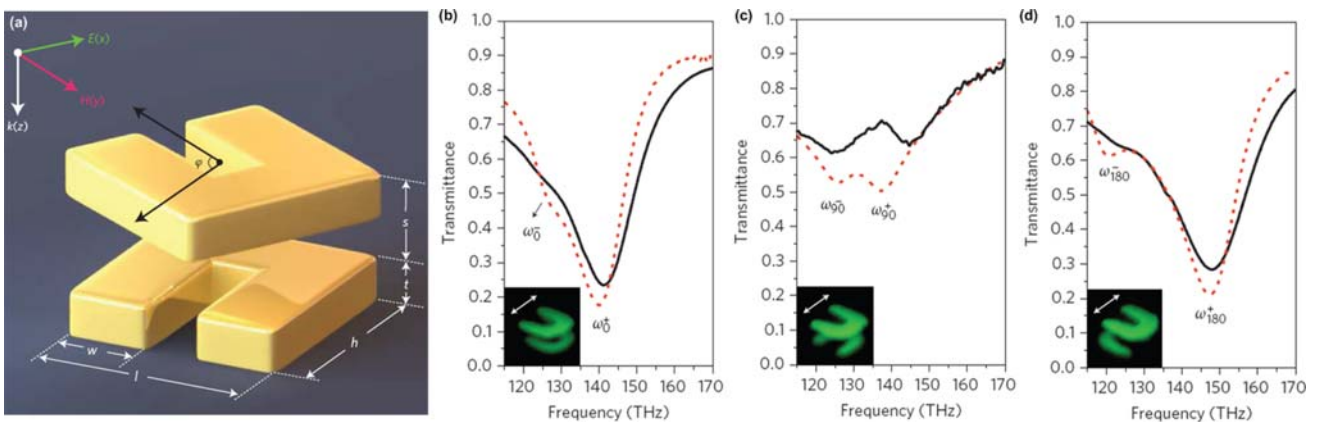

Figure 4 (online colour at: www.pss-b.com) (a) Schematic of the stereo-SRR dimer metamaterials twist angle φ. Experimental transmittance spectra for the 0° (b), 90° (c), and 180° (d) twisted SRR dimer metamaterials. The black and red curves represent the experimental and simulated results, respectively.

Feature

Article

Phys. Status Solidi B **246**, No. 7 (2009)   1401

In another work by Giessen and colleagues, the hybridization effect of an MP was also observed in four stacked SRRs [40]. In addition to in identical resonators, hybrid MP modes were found in coupled structures composed of different resonators, including SRR pairs [41], cut-wire pairs [42], tri-rods [43], and nanosandwiches in defective photonic crystals [44]. These hybrid MP modes could lead to some new interesting and useful properties, such as optical activity [37, 38] and omni-directional broadband negative refraction [43].

3 Magnetic plasmon waves in one-dimensional structures In the above section, we presented the hybridization effect of MP modes among several coupled magnetic resonators. In this section, we will generalize the theoretical model to one-dimensional infinite chains of coupled magnetic resonators. We will show that the collective excitation of infinite magnetic atoms in metamaterials can induce a new kind of wave, namely, an MP wave.

Linear chains of closely spaced metal nanoparticles have been intensely studied in recent years. Due to the strong near-field coupling interaction among these nanoparticles, a coupled electric plasmon propagation mode can be established in this chain and can be used to transport EM energy in a transverse dimension that is considerably smaller than the corresponding wavelength of illumination [45–50]. As this system can overcome the diffractive limit, it can function as a novel kind of integrated sub-wavelength waveguide.

According to the classic electrodynamics theory, the radiation loss of a magnetic dipole is substantially lower than the radiation of an electric dipole of a similar size [51]. Thus, using MP to guide EM energy over long distances has great potential for direct application in novel sub-diffraction-limited transmission lines without significant radiation losses.

Indeed, MP resonance has been already applied to a one-dimensional sub-wavelength waveguide in the microwave range [52–54]. Shamonina et al. proposed a propagation of waves supported by capacitively loaded loops using a circuit model in which each loop is coupled magnetically to a number of other loops [52]. Since the coupling is due to induced voltages, the waves are referred to as magneto-inductive waves (MI). The 1-D axial structure of the designed capacitively loaded loops is shown in Fig. 5(a), and the calculated dispersion curves for the wave vector *k* and attenuation coefficient α are given in Fig. 5(b)–(c). MI waves propagating on such 1-D lines may exhibit both forward and backward waves depending on whether the loops are arranged in an axial or planar configuration. Moreover, the band broadening could be obtained due to the excitation of MI waves, and the bandwidth changes dramatically as we vary the coupling coefficient between the resonators [55]. A kind of polariton mode could be formed by the interaction between the electromagnetic and MI waves, resulting in a tenability of the range where μ becomes negative [54]. In a biperiodic chain of magnetic
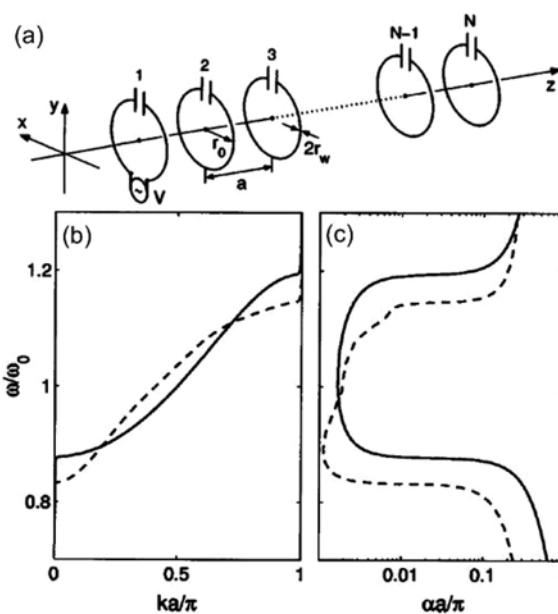

Figure 5 (a) 1-D axial structure of capacitively loaded loops. (b, c) Dispersion curves for the 1-D axial structure: nearest neighbor interactions only (solid line), interactions between 5 neighbors (dashed line).

resonators, the dispersion of the MI wave will be split into two branches analogous to acoustic waves in solids, and this can be used to obtain specified dispersion properties [56, 57]. In addition to this kind of MI wave, electro-inductive (EI) waves were also reported in the microwave range [58]. Further, the coupling may be either of the magnetic or electric type, depending on the relative orientation of the resonators. This causes the coupling constant between resonators to become complex and leads to even more complicated dispersion [59]. Up to now, a series of microwave devices based on MI waves have been proposed, such as magneto-inductive waveguides [60], broadband phase shifters [61], parametric amplifiers [62], and pixel-to-pixel sub-wavelength imagers [63, 64].
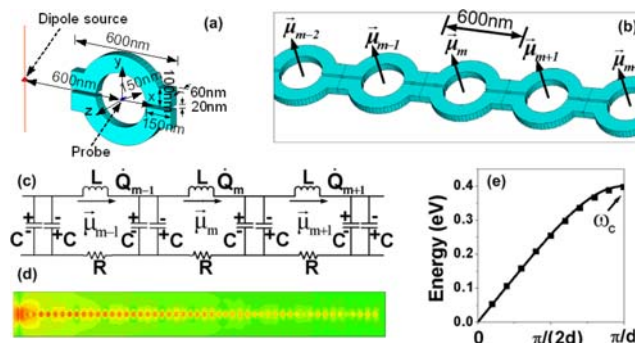

Figure 6 (online colour at: www.pss-b.com) (a) Structure of a single SRR; (b) one-dimensional chain of SRRs; (c) equivalent circuit of the chain; (d) FDTD simulation of MP wave propagation along the chain; (e) dispersion curve of the MP wave.

However, in the optical range, the ohmic loss inside metallic structures is much higher than in the microwave range. The MI coupling between the elements is not strong enough to transfer the energy efficiently. In order to improve the properties of the guided MP wave, the exchange current interaction between two connected SRRs is proposed [65], which is much stronger than the corresponding MI coupling.

Figure 6(b) shows one infinite chain of SRRs constructed by connecting the unit elements (see Fig. 6(a)) one by one. The magnetic dipole model can be applied to investigate this structure. If a magnetic dipole, μ_m, is assigned to each resonator and only nearest neighbor interactions are considered, then the Lagrangian and the dissipation function of the system can be written as

$$\mathfrak{I} = \sum_m \left(\frac{1}{2} L \dot{q}_m^2 - \frac{1}{4C} (q_m - q_{m+1})^2 + M \dot{q}_m \dot{q}_{m+1} \right),$$

$$\mathfrak{R} = \sum_m \frac{1}{2} \gamma \dot{q}_m^2 . \tag{6}$$

Substitution of Eq. (6) in the Euler−Lagrangian equations yields the equations of motion for the magnetic dipoles

$$\ddot{\mu}_m + \omega_0^2 \mu_m + \Gamma \dot{\mu}_m$$
$$= \frac{1}{2} \kappa_1 \omega_0^2 (\mu_{m-1} + 2\mu_m + \mu_{m+1}) - \kappa_2 (\ddot{\mu}_{m-1} + \ddot{\mu}_{m+1}), \tag{7}$$

where κ_1 and κ_2 are the coefficients of the exchange current and MI interactions respectively. The general solution of Eq. (7) corresponds to an attenuated MP wave: $\mu_m = \mu_0 \exp(-m\alpha d) \exp(i\omega t - imkd)$, where ω and k are the angular frequency and wave vector, respectively, α is the attenuation per unit length, and d is the size of the SRR. By substituting $\mu_m(t)$ into Eq. (7) and working in a small damping approximation ($\alpha d \ll 1$), simplified relationships for the MP dispersion and attenuation are obtained:

$$\omega^2(k) = \omega_0^2 \frac{1 - \kappa_1 [1 + \cos(kd)]}{1 + 2\kappa_2 \cos(kd)} . \tag{8}$$

In Fig. 6(e), numerically and analytically estimated MP dispersion properties are depicted as dots and solid curves respectively. In contrast to the electric plasmon modes in a linear chain of nanosized metal particles where both transverse and longitudinal modes can exist, the magnetic plasmon is exclusively a transversal wave. It is manifested by a single dispersion curve that covers a broad frequency range, $\omega \in (0, \omega_c)$, with the cutoff frequency $\hbar \omega_c \approx 0.4$ eV. Finally, it is important to mention that the MP properties can be tuned by changing the material used and the size and shape of the individual SRRs. Generally, the MP resonance frequency increases linearly with the decrease in the overall SRR size. However, the saturation of the magnetic response of the SRR at high frequen-

cies prevents this structure from achieving high-frequency operation [66]. In addition, the complicated shape and narrow gap of the SRRs make experiments very challenging.

The nanorod [67], nanosandwich [68], and slit-hole resonator (SHR) [69] are good alternatives to make sub-wavelength waveguides because of their simple structures and high working-frequency regime. Figure 7(a) presents the geometry of a single nanosandwich, composed of two equal-sized gold nanodiscs and a dielectric middle layer. Such a magnetic atom can also be used to construct a linear magnetic chain (Fig. 7(b)). Due to the near-field electric and magnetic coupling interactions, the MP propagation mode is established in this 1-D system. When excited by an EM wave, a strong local magnetic field is obtained in the middle layer at a specific frequency (Fig. 7(c)). For this magnetic plasmon resonance mode, the corresponding electric fields are given in Fig. 7(d). Through a Fourier transform method, the wave vectors of this MP wave at different EM wave frequencies are calculated. Then, the MP wave's dispersion property is obtained (shown as a white line in Fig. 7(e)). The light line in free space is also given as the black dotted line in the figure. The MP curve is divided into two parts by the light line. The part above the light line corresponds to bright MP modes whose energy can be radiated out from the chain, while the part below the light line corresponds to dark MP modes whose energy can be well confined within the chain. It is easy to see that the bright MP modes are much weaker than the dark MP modes for their leaky property. Therefore, only those EM waves in the frequency range of the dark MP modes can be transferred efficiently without radiation loss. The above results for a mono-periodic chain of nanosandwiches have been generalized to graded structures [70]. Some new interesting properties, such as slow group velocity and band folding of MP waves, are found in these more complex structures.
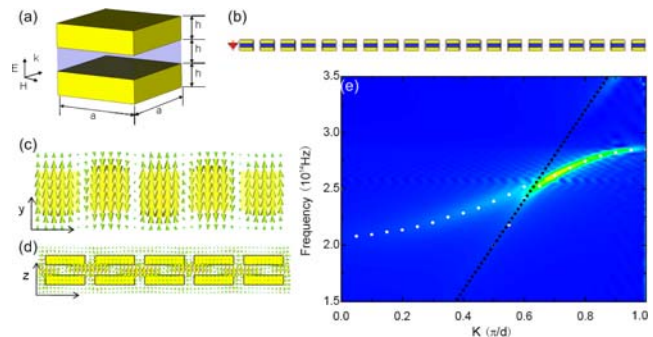

Figure 7 (online colour at: www.pss-b.com) (a) Structure of a single nanosandwich; (b) one-dimensional chain of nanosandwich; (c) electric field and (d) magnetic field of the MP wave propagation along the chain; (e) dispersion curve of the MP wave.
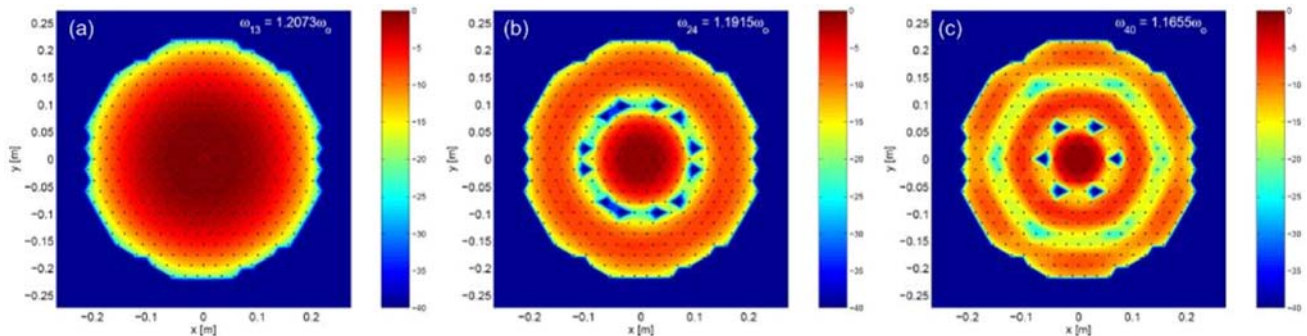
Phys. Status Solidi B **246**, No. 7 (2009)

Feature
Article

1403

Figure 8 (online colour at: www.pss-b.com) Current distributions for circular boundary conditions at various frequencies (a–c).

4 Excitation of magnetic plasmon polariton in two-dimensional structures In addition to the above-mentioned 1-D structures, the MP mode introduced by the coupling effect in 2-D systems is also an interesting topic. For 2-D metamaterials, the most important applications are negative refraction, focusing, and superlensing. How do the coupling interactions between elements affect the above processes? They cannot be handled by the conventional effective medium theory.

In the microwave range, MI wave theory has been proposed to deal with the coupling effect in the 2-D system. An MI superlens was proposed based on employing the coupling between resonators [63, 64], which eliminates the weakness of Wiltshire's first Swiss-roll superlens [12, 13] and has potential for MRI applications. The focusing of indefinite media, originally treated by Smith [71], has been investigated by Kozyrev with the aid of MI wave theory. It was found that partial focusing and multiple transmitted beams can be formed by the excitation of MI waves [72]. A further comparison between effective medium theory and MI wave theory was also given by Shadrivov [55], in which the reflection and refraction of MI waves on the boundary of two different effective media were studied. It was shown that both positive and negative refraction may occur under some configurations of the elements [73]. Another interesting finding is that spatial resonances could be formed by the propagation of MI waves on a 2-D array of magnetic resonators [74]. Different boundary conditions will produce different current and magnetic field distributions. For example, Fig. 8(a)–(c) gives the current distributions for circular boundary conditions at various frequencies.

In the optical frequency range, fishnet structures are well-known magnetic metamaterials [20], constructed by a metal/insulator/metal (MIM) sandwich with perforated periodic nanohole arrays. The fundamental physics to realize the negative permeability in this structure is based on the artificial magnetic atoms that consist of the magnetically exited LC-resonance between the two coupled metallic layer segments. In fishnet structures, all of these resonance elements are connected together, and strong exchange current interactions exist between them. Due to this strong coupling effect, MP waves with strong dispersion can be excited in the 2-D plane (double-fishnet) or 3-D bulk (multilayer-fishnet) structures.

For the 1-D system discussed in last section, the MP waves are confined within the chain of SRRs and have only one possible propagation direction. However, for the planar double-fishnet structures, MP waves can propagate in any direction on this plane. Therefore, the excitation MP waves in these 2-D systems are much more complex compared with in the 1-D system. Analogous to the polariton modes in MI waves [54], when the MP wave inside the fishnet structure is coupled with the incident electromagnetic waves, a new kind of polariton can be formed: a magnetic plasmon polariton (MPP).

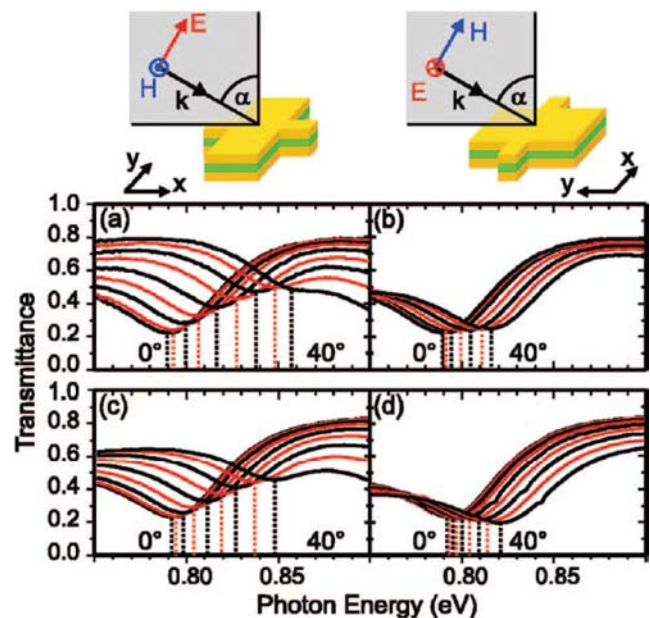In 2006, Dolling et al. observed the transmission dip induced by the excitation of an MPP in such a double-

Figure 9 (online colour at: www.pss-b.com) (a) and (b) Measured oblique-incidence transmittance spectra for different incident angles with respect to the surface normal, from 0° to 40° in steps of 5° (for clarity, the color alternates between black and red). The geometry is indicated on the top. (c) and (d) Calculated spectra corresponding to (a) and (b), respectively.
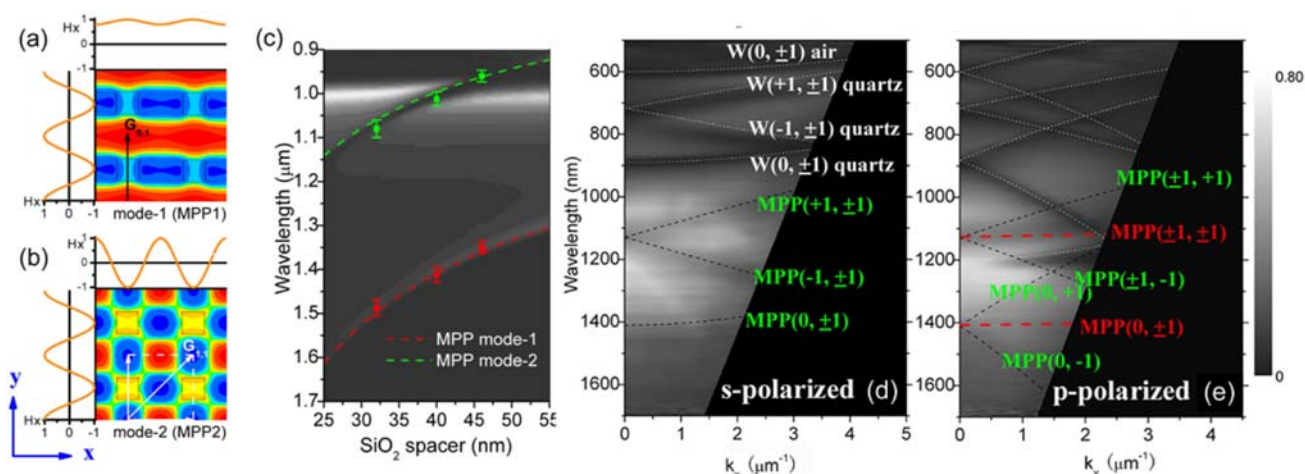
Figure 10 (online colour at: www.pss-b.com) Results of fishnet with square hole: (a) Simulated magnetic field distribution for mode 1 (a) and for mode 2 (b) in the middle SiO$_2$ layer of fishnet; (c) calculated transmittance map of fishnet as middle layer thickness ranging from 25 nm to 55 nm. Results of fishnet with rectangular hole: measured transmission maps on an intuitive gray scale versus wavelength and wavevectors for (d) s-polarization and (e) p-polarization.

fishnet structure [75]. By measuring and calculating the oblique-incidence transmittance spectra of this system, the authors inferred the in-plane dispersion relation of the magnetization wave (see Fig. 9). From the geometry and the dispersion shape, the authors conclude that coupling is predominantly via magnetic dipoles for waves propagating along the magnetic-dipole direction. These magnetization waves are the classical analogue of magnon excitations of quantum-mechanical spins.

What they observed is essentially only the lowest mode of the MPP. In the following, multiple MPP modes related to the reciprocal vectors of the array lattice were convincingly demonstrated [76]. Figure 10(a)–(b) show the magnetic field distributions of two mentioned MPP modes associated with the reciprocal vectors of $G(0, 1)$ and $G(1, 1)$. Figure 10(c) is a calculated transmission map with the SiO$_2$ layer thickness ranging from 25 nm to 55 nm, where two MPP modes and SPP modes are clearly exhibited.

Afterward, we also studied the dispersion properties of the MPP modes in the fishnet structure with rectangular hole arrays [77]. By careful investigation of the transmission property on the oblique incidence for the s- and p-polarization cases, we found a polarization-dependent dispersion property of the concerned MPP modes, which was indicated in the transmission maps for these two polarizations, as shown in Fig. 10(d)–(e). From this, we can see that the MPP(1, 1) mode in the s-polarization actually exhibits much larger dispersions than the lowest mode, resulting in two split modes MPP(+1, 1) and MPP(−1, 1) that break the degeneration. This is very similar to the property of SPP in plasmonic crystals. As for the anisotropic properties, we can attribute them to different coupling intensities among the artificial magnetic atoms in different directions. In brief, the MPP excitations in the fishnet are not the behavior of a single isolated element. Instead, they come from the coupling effect between the artificial mag-

netic atoms, which are the delocalized mode in the fishnet structures [78]. This MPP offers another way to tailor the optical property in addition to the SPP-enhanced extraordinary transmissions.

5 Outlook Although metamaterials composed of uncoupled magnetic resonance elements have been successfully applied to produce intriguing effects such as negative refraction, cloaking, and superlensing, all of these were devised within a very narrow frequency range around a specific resonance frequency. This disadvantage restricts the practical applications of metamaterials.

In addition to the abovementioned applications of the linear optical effect, due to the great enhancement of the local field inside magnetic resonators, magnetic metamaterials have also been proposed for use in nonlinear optical processes, such as SERS [5], SHG [79, 80], nanolasers [81], and SPASER [82]. However, the nonlinear optical processes that occur between waves of several different frequencies typically require a broad frequency bandwidth. The narrow single resonance property of conventional metamaterials is a considerable disadvantage for their potential nonlinear optical applications.

The MP modes introduced by the coupling effect in metamaterials may provide a possible way to overcome the abovementioned obstacle. As described in this paper, hybrid MP resonance modes could be attained in a system with several coupled resonators. This hybridization effect results in multiple discrete resonance frequencies of magnetic metamaterials. When all the resonance elements in metamaterials are coupled together through a particular method, the multiple resonance levels will be extended to a continuous frequency band. Therefore, the excitation of MP modes in such metamaterials can be continually tuned within a rather wide range. Compared with conventional metamaterials made from uncoupled elements, this kind of

Phys. Status Solidi B **246**, No. 7 (2009)

1405

Feature

Article

broadband tunable magnetic metamaterial based on the coupling effect will have much more interesting and prospective applications, especially on the nonlinear optical effect. Based on this discussion, we anticipate that many novel metamaterials and nanophotonic devices will be developed from coupled resonator systems.

References

[1] V. G. Veselago, Sov. Phys. Usp. **10**, 509 (1968).
[2] J. Brown, Proc. IEE C **100**, 51 (1953).
[3] W. Rotman, IRE Trans. Antennas Propag. **10**, 82 (1962).
[4] J. B. Pendry, A. J. Holden, W. J. Stewart, and I. Youngs, Phys. Rev. Lett. **76**, 4773 (1996).
[5] J. B. Pendry, A. J. Holden, D. J. Robbins, and W. J. Stewart, IEEE Trans. Microw. Theory Tech. **47**, 2075 (1999).
[6] D. R. Smith, W. J. Padilla, D. C. Vier, S. C. Nemat-Nasser, and S. Schultz, Phys. Rev. Lett. **84**, 4184 (2000).
[7] R. A. Shelby, D. R. Smith, and S. Schultz, Science **292**, 77 (2001).
[8] J. B. Pendry, Phys. Rev. Lett. **85**, 3966 (2000).
[9] N. Fang, H. Lee, C. Sun, and X. Zhang, Science **308**, 534 (2005).
[10] Z. W. Liu, H. Lee, Y. Xiong, C. Sun, and X. Zhang, Science **315**, 1686 (2007).
[11] X. Zhang and Z. W. Liu, Nature Mater. **7**, 435 (2008).
[12] M. C. K. Wiltshire, J. B. Pendry, I. R. Young, D. J. Larkman, D. J. Gilderdale, and J. V. Hajnal, Science **291**, 849 (2001).
[13] M. C. K. Wiltshire, J. V. Hajnal, J. B. Pendry, D. J. Edwards, and C. J. Stevens, Opt. Express **11**, 709 (2003).
[14] T. J. Yen, W. J. Padilla, N. Fang, D. C. Vier, D. R. Smith, J. B. Pendry, D. N. Basov, and X. Zhang, Science **303**, 1494 (2004).
[15] S. Linden, C. Enrich, M. Wegener, J. F. Zhou, T. Koschny, and C. M. Soukoulis, Science **306**, 1351 (2004).
[16] C. Enrich, M. Wegener, S. Linden, S. Burger, L. Zschiedrich, F. Schmidt, J. F. Zhou, T. Koschny, and C. M. Soukoulis, Phys. Rev. Lett. **95**, 203901 (2005).
[17] Y. Svirko, N. Zheludev, and M. Osipov, Appl. Phys. Lett. **78**, 498 (2001).
[18] V. A. Podolskiy, A. K. Sarychev, and V. M. Shalaev, J. Nonlin. Opt. Phys. Mater. **11**, 65 (2002).
[19] V. M. Shalaev, W. S. Cai, U. K. Chettiar, H. K. Yuan, A. K. Sarychev, V. P. Drachev, and A. V. Kildishev, Opt. Lett. **30**, 3356 (2005).
[20] S. Zhang, W. J. Fan, N. C. Panoiu, K. J. Malloy, R. M. Osgood, and S. R. J. Brueck, Phys. Rev. Lett. **95**, 137404 (2005).
[21] J. Yao, Z. W. Liu, Y. M. Liu, Y. Wang, C. Sun, G. Bartal, A. M. Stacy, and X. Zhang, Science **321**, 930 (2008).
[22] J. Valentine, S. Zhang, T. Zentgraf, E. Ulin-Avila, D. A. Genov, G. Bartal, and X. Zhang, Nature **455**, 376 (2008).
[23] J. B. Pendry, Contemp. Phys. **45**, 191 (2004).

[24] J. B. Pendry, Nature Mater. **5**, 599 (2006).
[25] V. M. Shalaev, Nature Photon. **1**, 41 (2007).
[26] C. M. Soukoulis, S. Linden, and M. Wegener, Science **315**, 47 (2007).
[27] V. G. Veselago and E. E. Narimanov, Nature Mater. **5**, 759 (2006).
[28] J. B. Pendry, D. Schurig, and D. R. Smith, Science **312**, 1780 (2006).
[29] D. Schurig, J. J. Mock, B. J. Justice, S. A. Cummer, J. B. Pendry, A. F. Starr, and D. R. Smith, Science **314**, 977 (2006).
[30] R. Liu, C. Ji, J. J. Mock, J. Y. Chin, T. J. Cui, and D. R. Smith, Science **323**, 366 (2009).
[31] E. Prodan, C. Radloff, N. J. Halas, and P. Nordlander, Science **302**, 419 (2003).
[32] E. Prodan and P. Nordlander, J. Chem. Phys. **120**, 5444 (2004).
[33] P. Nordlander, C. Oubre, E. Prodan, K. Li, and M. I. Stockman, Nano Lett. **4**, 899 (2004).
[34] D. W. Brandl, C. Oubre, and P. Nordlander, J. Chem. Phys. **123**, 024701 (2005).
[35] C. Oubre and P. Nordlander, J. Chem. Phys. B **109**, 10042 (2005).
[36] P. Nordlander and E. Prodan, Nano Lett. **4**, 2209 (2004).
[37] H. Liu, D. A. Genov, D. M. Wu, Y. M. Liu, Z. W. Liu, C. Sun, S. N. Zhu, and X. Zhang, Phys. Rev. B **76**, 073101 (2007).
[38] T. Q. Li, H. Liu, T. Li, S. M. Wang, F. M. Wang, R. X. Wu, P. Chen, S. N. Zhu, and X. Zhang, Appl. Phys. Lett. **92**, 131111 (2008).
[39] N. Liu, H. Liu, S. N. Zhu, and H. Giessen, Nature Photon. **3**, 157 (2009).
[40] N. Liu, H. C. Guo, L. W. Fu, S. Kaiser, H. Schweizer, and H. Giessen, Nature Mater. **7**, 31 (2008).
[41] H. C. Guo, N. Liu, L. W. Fu, T. P. Meyrath, T. Zentgraf, H. Schweizer, and H. Giessen, Opt. Express **15**, 12095 (2007).
[42] N. Liu, H. C. Guo, L. W. Fu, S. Kaiser, H. Schweizer, and H. Giessen, Adv. Mater. **19**, 3628 (2007).
[43] F. M. Wang, H. Liu, T. Li, S. N. Zhu, and X. Zhang, Phys. Rev. B **76**, 075110 (2007).
[44] D. Y. Lu, H. Liu, T. Li, S. M. Wang, F. M. Wang, S. N. Zhu, and X. Zhang, Phys. Rev. B **77**, 214302 (2008).
[45] M. Quinten, A. Leitner, J. R. Krenn, and F. R. Aussenegg, Opt. Lett. **23**, 1331 (1998).
[46] M. L. Brongersma, J. W. Hartman, and H. A. Atwater, Phys. Rev. B **62**, 16356 (2000).
[47] S. A. Maier, P. G. Kik, and H. A. Atwater, Phys. Rev. B **67**, 205402 (2003).
[48] W. H. Weber and G. W. Ford, Phys. Rev. B **70**, 125429 (2004).
[49] C. R. Simovski, A. J. Viitanen, and S. A. Tretyakov, Phys. Rev. E **72**, 066606 (2005).
[50] A. F. Koenderink and A. Polman, Phys. Rev. B **74**, 033402 (2006).
[51] J. D. Jackson, Classical Electrodynamics (Wiley, New York, 1999).
[52] E. Shamonina, V. Kalinin, K. H. Ringhofer, and L. Solymar, J. Appl. Phys. **92**, 6252 (2002).
[53] M. J. Freire, R. Marques, F. Medina, M. A. G. Laso, and F. Martin, Appl. Phys. Lett. **85**, 4439 (2004).

[54] R. R. A. Syms, E. Shamonina, V. Kalinin, and L. Solymar, J. Appl. Phys. **97**, 064909 (2005).

[55] I. V. Shadrivov, A. N. Reznik, and Y. S. Kivshar, Physica B **394**, 180 (2007).

[56] O. Sydoruk, O. Zhuromskyy, E. Shamonina, and L. Solymar, Appl. Phys. Lett. **87**, 072501 (2005).

[57] O. Sydoruk, A. Radkovskaya, O. Zhuromskyy, E. Shamonina, M. Shamonin, C. J. Stevens, G. Faulkner, D. J. Edwards, and L. Solymar, Phys. Rev. B **73**, 224406 (2006).

[58] M. Beruete, F. Falcone, M. J. Freire, R. Marques, and J. D. Baena, Appl. Phys. Lett. **88**, 2006 (2006).

[59] F. Hesmer, E. Tatartschuk, O. Zhuromskyy, A. A. Radkovskaya, M. Shamonin, T. Hao, C. J. Stevens, G. Faulkner, D. J. Edwards, and E. Shamonina, Phys. Status Solidi B **244**, 1170 (2007).

[60] R. R. A. Syms, E. Shamonina, and L. Solymar, IEE Proc. Microw. Antennas Propag. **153**, 111 (2006).

[61] I. S. Nefedov and S. A. Tretyakov, Microw. Opt. Technol. Lett. **45**, 98 (2005).

[62] R. R. A. Syms, L. Solymar, and I. R. Young, Metamaterials **2**, 122 (2008).

[63] M. J. Freire and R. Marques, Appl. Phys. Lett. **86**, 182505 (2005).

[64] O. Sydoruk, M. Shamonin, A. Radkovskaya, O. Zhuromskyy, E. Shamonina, R. Trautner, C. J. Stevens, G. Faulkner, D. J. Edwards, and L. Solymar, J. Appl. Phys. **101**, 073903 (2007).

[65] H. Liu, D. A. Genov, D. M. Wu, Y. M. Liu, J. M. Steele, C. Sun, S. N. Zhu, and X. Zhang, Phys. Rev. Lett. **97**, 243902 (2006).

[66] J. Zhou, T. Koschny, M. Kafesaki, E. N. Economou, J. B. Pendry, and C. M. Soukoulis, Phys. Rev. Lett. **95**, 223902 (2005).

[67] F. M. Wang, H. Liu, T. Li, S. M. Wang, and S. N. Zhu, Appl. Phys. Lett. **91**, 133107 (2007).

[68] S. M. Wang, T. Li, H. Liu, F. M. Wang, S. N. Zhu, and X. Zhang, Opt. Express **16**, 3560 (2008).

[69] H. Liu, T. Li, Q. J. Wang, Z. H. Zhu, S. M. Wang, J. Q. Li, S. N. Zhu, Y. Y. Zhu, and X. Zhang, Phys. Rev. B **79**, 024304 (2009).

[70] S. M. Wang, T. Li, H. Liu, F. M. Wang, S. N. Zhu, and X. Zhang, Appl. Phys. Lett. **93**, 233102 (2008).

[71] D. R. Smith, P. Kolinko, and D. Schurig, J. Opt. Soc. Am. B **21**, 1032 (2004).

[72] A. B. Kozyrev, C. Qin, I. V. Shadrivov, Y. S. Kivshar, I. L. Chuang, and D. W. V. D. Weide, Opt. Express **15**, 11714 (2007).

[73] R. R. A. Syms, E. Shamonina, and L. Solymar, Eur. Phys. J. B **46**, 301 (2005).

[74] O. Zhuromskyy, E. Shamonina, and L. Solymar, Opt. Express **13**, 9299 (2005).

[75] G. Dolling, M. Wegener, A. Schadle, S. Burger, and S. Linden, Appl. Phys. Lett. **89**, 231118 (2006).

[76] T. Li, J. Q. Li, F. M. Wang, Q. J. Wang, H. Liu, S. N. Zhu, and Y. Y. Zhu, Appl. Phys. Lett. **90**, 251112 (2007).

[77] T. Li, S. M. Wang, H. Liu, J. Q. Li, F. M. Wang, S. N. Zhu, and X. Zhang, J. Appl. Phys. **103**, 023104 (2008).

[78] T. Li, H. Liu, F. M. Wang, J. Q. Li, Y. Y. Zhu, and S. N. Zhu, Phys. Rev. E **76**, 016606 (2007).

[79] M. W. Klein, C. Enkrich, M. Wegener, and S. Linden, Science **313**, 502 (2006).

[80] N. Feth, S. Linden, M. W. Klein, M. Decker, F. B. P. Niesler, Y. Zeng, W. Hoyer, J. Liu, S. W. Koch, J. V. Moloney, and M. Wegener, Opt. Lett. **33**, 1975 (2008).

[81] A. K. Sarychev and G. Tartakovsky, Phys. Rev. B **75** (2007).

[82] N. I. Zheludev, S. L. Prosvirnin, N. Papasimakis, and V. A. Fedotov, Nature Photon. **2**, 351 (2008).